Infrared Matrix Isolation Studies of the Reactions of Dichloro- and Dibromomethane with Atomic Oxygen

C. Lugez, A. Schriver, and L. Schriver-Mazzuoli*

Laboratoire de Physique Moléculaire et Applications, CNRS UPR 136, Université Pierre et Marie Curie, Tour 13, Bte 76, 4 Place Jussieu 75252 Paris Cedex 05, France

E. Lasson and C. J. Nielsen

Department of Chemistry, University of Oslo, P.O. Box 1033 Blindern, N-0315 Oslo, Norway

Received: June 21, 1993; In Final Form: August 23, 1993®

The reactions of atomic oxygen with CH_2Cl_2 and CH_2Br_2 trapped in argon matrices have been studied by FTIR spectroscopy. $O(^1D)$ and $O(^3P)$ were generated *in situ* by UV photolysis of co-deposited ozone. Products were identified by employing ^{18}O and scrambled $^{18}O/^{16}O$ ozone as well as deuterated methylene halides. Kinetic studies performed on both CH_2Cl_2 and CH_2Br_2 with $O(^1D)$ under the same experimental conditions allowed the reaction pathways to be determined. With CH_2Br_2 as parent molecule, three routes were evident leading to (i) CHOBr, (ii) $CO\cdots(HBr)_2$, and (iii) CH_2O. With CH_2Cl_2 as parent molecule, only the first two channels were observed. Carbonyl compounds rapidly decomposed under irradiation, and $CO\cdots(HX)_2$ was also produced as a secondary species.

Introduction

The Airborne Antarctic Ozone Experiment, conducted in 1987, showed that depletion of polar ozone is caused by extremely high levels of ClO derived from industrial chlorofluorocarbons with significant contributions from BrO derived from both natural and industrial sources.[1] Very high levels of ClO and enhanced concentrations of BrO were also detected in the Arctic during the first Airborne Arctic Stratospheric Expedition (AASE-I) carried out in 1989.[2] It is known that the ozone loss each spring over Antarctica is in large part caused by chlorine and bromine catalysis and also that the enhanced chlorine catalysis results from the alteration of the chemical environment near and inside the polar vortex by heterogeneous processes.[3] It is therefore important to obtain a detailed knowledge of all the different atmospheric degradation mechanisms of halogenated hydrocarbons.

In this paper, we present results from infrared matrix isolation (IRMI) studies of the chemical reaction of dichloro- and dibromomethane with oxygen atoms. Some partial results for the $CH_2Br_2 + O_3$ reaction have recently been presented,[4] but the aim of the present paper is to compare the reactivity of CH_2Cl_2 and CH_2Br_2 under the same irradiation conditions. These compounds were mainly chosen as model compounds for more complex halocarbons, but they also occur themselves in the atmosphere. Dichloromethane has a tropospheric concentration of approximately 35 pptv and a lifetime of half a year. The bromo compound has a tropospheric concentration of only 2–3 pptv.[3] Even though this is a very low value, it is known that bromine in extremely low concentrations can enhance the ozone depletion by up to 20%.[5]

The results will be discussed in comparison with those obtained in our previous studies concerning the reaction of oxygen atoms with $CBrCl_3$,[6] $CHCl_3$,[7] and $CFCl_3$.[8]

Experimental Section

The samples of CH_2Cl_2 and CH_2Br_2 were standard *p.a.* laboratory reagents, while the deuterated samples originated from Eurisotop and MSD, respectively. The samples were purified by distillation and checked by GC–MS before use. Ozone was prepared from oxygen by electrical discharge in a closed system and trapped in liquid nitrogen. ^{18}O-enriched samples of ozone were prepared from 96 atom % $^{18}O_2$ and 50 atom % $^{18}O_2$ originating from ICN Biomedicals and Eurisotop. Unfortunately, our ozone samples invariably contained traces of CO and CO_2.

The matrix isolation spectra were recorded using two different experimental arrangements: The Paris system consisted of a Model 202A closed-cycle displex unit from Air Products equipped with a gold-plated mirror and a Bruker IFS 113v FTIR working in reflection mode. The Oslo System consisted of the same type of displex unit but was set up for transmission measurements employing a Bruker IFS 88. The samples were mixed with argon by standard nanometric methods and sprayed onto the 20 K cold mirror/window using dual-nozzle systems, and the spectra were subsequently recorded at 10 K with 0.5-cm^{-1} resolution (Paris) and at 15 K with 1-cm^{-1} resolution (Oslo).

The deposited sample mixtures were irradiated with the UV light from medium-pressure mercury lamps. Some photolysis experiments were performed without optical filters. However, in most of the experiments a 280-nm cut-off filter was inserted to prevent photolysis of the parent halide as well as possible secondary photolysis. With this filter, both $O(^3P)$ and $O(^1D)$ are formed from ozone, but experiments were also carried out employing a 360-nm filter whereby only $O(^3P)$ results.

An experiment was performed with dichloromethane in solid oxygen (1/1000). The photolysis was performed with the full output of a mercury lamp. Irradiation of solid O_2 with UV irradiation below 280 nm produces ozone and $O(^3P)$ followed by subsequent secondary photolysis of the ozone producing both states of atomic oxygen.

Results

Vibrational Spectra of the Parent Molecules. The observed fundamental bands of matrix-isolated CH_2Cl_2, CD_2Cl_2, CH_2Br_2, and CD_2Br_2 have been collected in Tables I and II, which also contain data from earlier vapor-phase[9,10] and matrix isolation[11–15] studies. After a short annealing of the matrices to 25 K, new bands appeared near the original bands, *i.e.*, for CH_2Cl_2: 3053 (ν_6), 2992.4 (ν_1), 1423.4–1421.2 (ν_2), 1268.7 (ν_8), 1160 (ν_5), 746.5–748.5 (ν_9), and 712.5–709.4 cm^{-1} (ν_3). The same bands were also

* Author to whom correspondence should be addressed.
® Abstract published in *Advance ACS Abstracts*, October 1, 1993.

0022-3654/93/2097-11617$04.00/0

TABLE I: Comparison of Fundamental Vibration Frequencies (in cm^{-1}) for Isotopic Methylene Chlorides in Vapor Phase and Argon Matrix. Observed and Calculated Frequency Shifts (in cm^{-1})

		vapor-phase data[a]			argon matrix data			
		$^{12}CH_2{}^{35}Cl^{35}Cl$	$\Delta(^{12}CH_2{}^{35}Cl^{37}Cl)$	$\Delta(^{12}CH_2{}^{37}Cl^{37}Cl)$[d]	Andrews	Mikulec	King	this work
A_1	ν_1	2997.66	0.0	0.0	2998	2993		2993.6 (0.2)
	ν_2	1435.0	0.0	0.0		1423[c]		1428.4 (0.07)
	ν_3	712.9	−2.9	−6.0		710/706/704	712.9/709.1/706.6	711.6/708.7/706.1 (0.28/0.2/0.05)
	ν_4	281.5[b]	−3.4	−6.8				
A_2	ν_5	1153[b]	−0.2	−0.3				1156.8 (0.03)
B_1	ν_6	3055[b]	0.0	0.0		3059		3056 (0.001)
	ν_7	898.66	−0.3	−0.6		894		894.4 (0.11)
B_2	ν_8	1268.86	−0.2	−0.3	1276	1265		1266.2 (1)
	ν_9	759.82	−2.2	−4.8	747	747/746/744	749.3/747.3/744.4	749.3/746.0/744.0 (0.88/0.68/0.11)

		$^{12}CD_2{}^{35}Cl^{35}Cl$	$\Delta(^{12}CD_2{}^{35}Cl^{37}Cl)$	$\Delta(^{12}CD_2{}^{37}Cl^{37}Cl)$[d]	Andrews	this work
A_1	ν_1	2205.65	0.0	−0.0	2205	2202.6 (0.09)
	ν_2	1060.81	0.0	−0.0		1055.6 (0.01)
	ν_3	687.6	−3.1	−6.4		685.3/682.1/679.4 (0.1/0.09/0.03)
	ν_4	279[b]	−3.1	−6.6		
A_2	ν_5	825	−0.2[d]	−0.5		826.9 (0.013)
B_1	ν_6	2303.72	0.0	0.0		2304.0 (0.001)
	ν_7	713[b]	−0.4	−0.8		707.2/704.8 (0.013/0.011)
B_2	ν_8	961.04	−0.1[d]	−0.1	957	956.2/955.1 (0.47/0.44)
	ν_9	730.26	−2.9	−5.4	723	721/719.4/716.6 (1/0.98/0.17)

[a] Reference 19. [b] Reference 30. [c] Changed assignment. [d] Calculated (see text).

TABLE II: Comparison of Fundamental Vibration Frequencies (in cm^{-1}) for Isotopic Methylene Bromides in Vapor Phase and Argon Matrix. Observed and Calculated Frequency Shifts (in cm^{-1})

		vapor-phase data[a]			argon matrix data			
		$^{12}CH_2{}^{79}Br^{79}Br$	$\Delta(^{12}CH_2{}^{79}Br^{81}Br)$[d]	$\Delta(^{12}CH_2{}^{81}Br^{81}Br)$[d]	Kelsall	Andrews	Young	this work
A_1	ν_1	3009	0.0	0.0		3011		3005.5 (0.006)
	ν_2	1382	0.0	0.0				1400.1 (0.005)
	ν_3	588	−0.6	−1.1	582.97/582.44/581.92			583.0 (0.04)
	ν_4	169[b]	−1.1	−2.1				
A_2	ν_5	1095[c]	0.0	−0.7				1096.8 (0.007)
B_1	ν_6	3073	0.0	0.0			3074	3073 (0.007)
	ν_7	812	−0.1	−0.1			811.5	811.4 (0.05)
B_2	ν_8	1195	−0.8	−0.7		1195	1194.5	1194.2 (0.51)
	ν_9	653	−0.5	−1.0	649.41/648.96/648.48	650	649.0	648.9 (1.0)

		$\Delta(^{12}CD_2{}^{79}Br^{79}Br)$	$\Delta(^{12}CD_2{}^{79}Br^{81}Br)$[d]	$\Delta(^{12}CD_2{}^{81}Br^{81}Br)$[d]	Andrews	this work
A_1	ν_1	2214	0.0	0.0	2208	2204.7 (0.012)
	ν_2	1032	0.0	0.0		1034.1 (0.005)
	ν_3	559	−0.6	−1.2		555.4 (0.12)
	ν_4	172[b]	−1.0	−2.1		
A_2	ν_5	790	0.0	−0.1		781.5 (0.007)
B_1	ν_6	2324	0.0	0.0		2316.1 (0.015)
	ν_7	625	−0.1	−0.1		622.9 (0.22)
B_2	ν_8	907	0.0	0.0	905	903.0 (1.0)
	ν_9	608[c]	−0.5	−0.7	621	618.6 (0.92)

[a] Reference 10. [b] Raman liq. [c] Liquid phase. [d] Calculated (see text).

observed by increasing the CH_2Cl_2 concentration and have been attributed to molecular aggregates. In contrast to this, the IR spectra of co-deposited methylene halide and ozone showed no bands that could not be attributed to the parent molecules, and apparently there is no significant interaction between the two molecules.

The infrared spectra of matrix-isolated ozone and ^{18}O-substituted ozone have been studied extensively (refs 16–18 and references therein). Our spectra were in good agreement with the literature.

Vibrational Spectra after Photolysis. Preliminary experiments where matrix-isolated dichloro- and dibromomethane were exposed to prolonged UV irradiation with $\lambda > 250$ nm showed no detectable degradation of the samples.

After irradiation of a $CH_2Cl_2/O_3/Ar$ sample (1/3/800 ratio) for 2 h by the unfiltered light from the UV source, approximately half of the ozone had vanished, and at the same time several new features appeared around 2800, 2150, and 1750 cm^{-1} (Figure 1). The observed wavenumbers and optical densities are listed in Table III, which also contains the data obtained from experiments with isotopic species. The bands at 2811.2 and 2781.1 cm^{-1} shifted to 2035.4 and 2012.3 cm^{-1} with deuterium substitution. The three weak bands in the carbonyl region at 1756.7, 1754.6, and 1751.3 cm^{-1} (the latter the strongest of the three) were shifted to 1715.4, 1713.2, and 1710.1 cm^{-1}, respectively, when $^{18}O_3$ was used as precursor and to 1731.4 and 1724.4 cm^{-1} when the deuterated dichloromethane was used. When scrambled $^{18}O/^{16}O$ ozone was used as precursor, the spectrum revealed the same bands as in the separate $^{16}O_3$ and $^{18}O_3$ experiments and with equal intensities.

Temperature increase revealed different behavior of the triplet components in the carbonyl region as illustrated in Figure 2, where a sequence of temperature and photolysis effects is presented in a $CH_2Cl_2/^{16}O_3$ experiment. The feature at 1756 cm^{-1} turned out to disappear quickly upon UV photolysis—even when using the 280-nm filter—but reappeared as the temperature was increased above 30 K. After annealing at 40 K, it grew strongly accompanied by a new absorption at 1763 cm^{-1}. The weak component at 1754.6 cm^{-1} appeared insensitive to temperature increase, whereas the main component at 1751.3 cm^{-1} and also the 1756.7-cm^{-1} absorption showed an intensity increase with temperature.

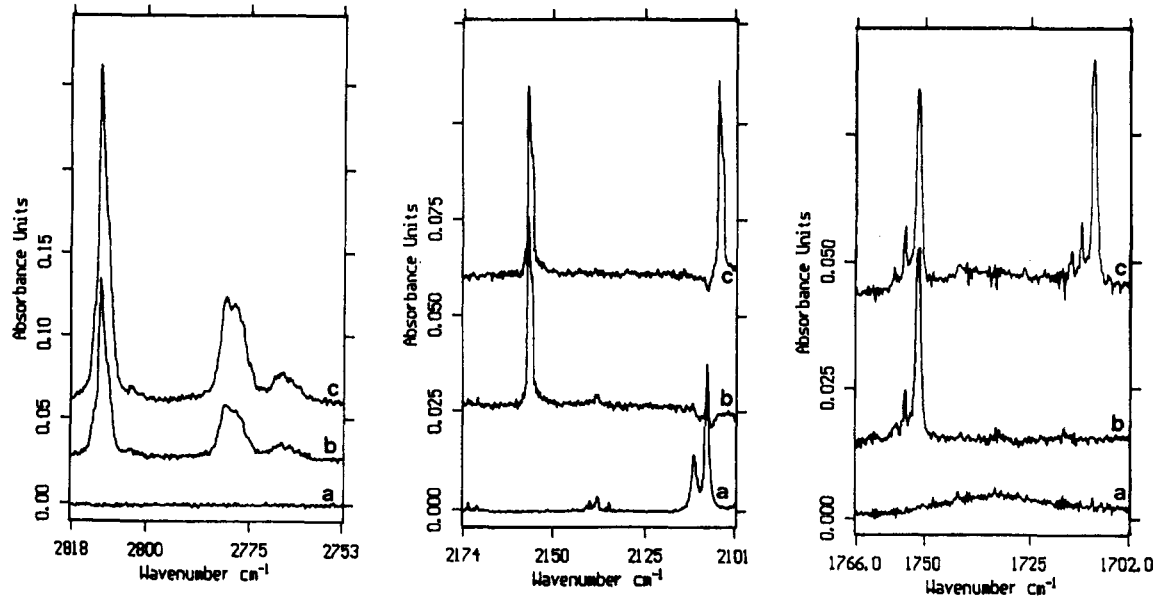

Figure 1. Detailed FTIR spectra of CH_2Cl_2 and natural and isotopic O atom matrix reaction products in the 2800–2750-, 2170–2100-, and 1765–1700-cm^{-1} regions: (a) after deposition at 20 K of $CH_2Cl_2/O_3/Ar$ = 1/1/1000 mixture, (b) $^{16}O_3$ after irradiation with the unfiltered medium-pressure mercury lamp for 1 h, and (c) $^{16-18}O_3$ (50%–50%) after irradiation with the filtered medium-pressure mercury lamp for 3 h. All spectra are recorded at 11 K.

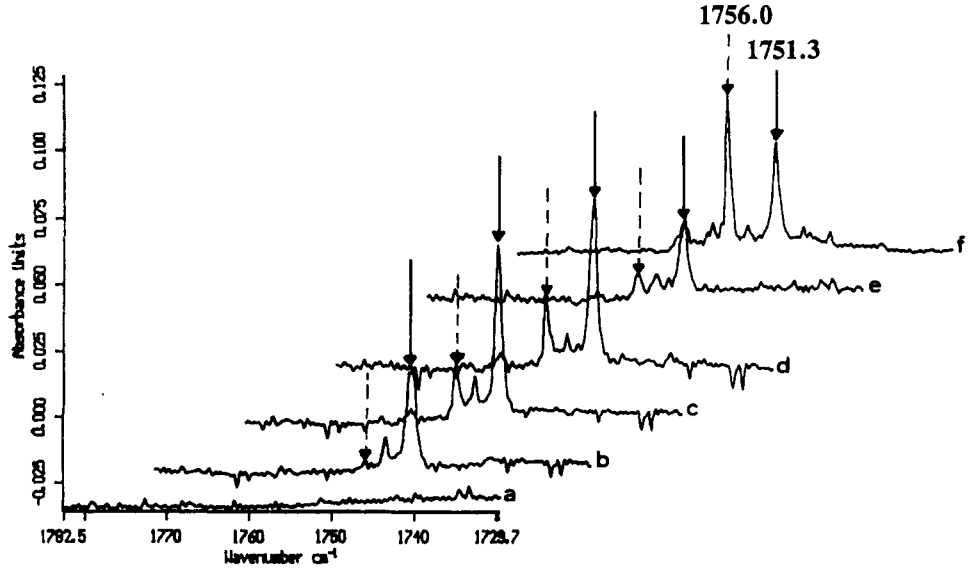

Figure 2. Temperature effects on the CH_2Cl_2 and O atom reaction products in the carbonyl region: (a) after deposition of $CH_2Cl_2/O_3/Ar$ = 1/2/1000, (b) after irradiation with medium-pressure mercury lamp and cut-off filter WG 280 for 1 h with recording temperature T_s = 11 K, (c) part b recording at 31 K, (d) part c recording at 12 K, (e) after second irradiation at 12 K with previous filter for 1 h and 30 min, and (f) part e after annealing at 40 K, recording at 11 K.

TABLE III: Main Absorptions (cm^{-1}) Formed after Medium-Pressure Mercury Lamp Irradiation of Argon Matrices Containing Natural or Isotopic Ozone and Hydrogenated, Deuterated Methylene Chloride[a]

$CH_2Cl_2 + {}^{16}O_3$	$CH_2Cl_2 + {}^{18}O_3$	$CD_2Cl_2 + {}^{16}O_3$	assignment
2811.2 (0.101)	2811.2	2035.4	ν(HCl), $(HCl)_2$···CO
2781.1 (0.03)	2781.1	2012.3	
2156.6 (0.08)	2105.3	2158.0	ν(CO), $(HCl)_2$···CO
2155.6 (0.03)			
1756.7 (0.004)	1715.4		
1754.6 (0.008)	1713.2	1731.4	ν(C=O),
1751.3 (0.04)	1710.1	1724.4	(HClC=O···HCl)

[a] In parentheses are peak height absorbance values for the $CH_2Cl_2 + {}^{16}O_3$ reaction; irradiation time: 4 h).

The analogous experiment with an argon matrix containing $CH_2Br_2/O_3/Ar$ in a 1/2/1000 mixing ratio and photolyzed for 1 h revealed new bands around 2500, 2150, and 1800–1700 cm^{-1} (Figure 3). The spectral features obtained from experiments with different isotopic species are summarized in Table IV. The bands at 2499.3 and 2484.8 cm^{-1} shifted to 1794.9 and 1784.8 cm^{-1}, respectively, when using the deuterated analogue. The four main bands in the carbonyl region appeared at 1799.5, 1756.3–1754.9, 1742.5, and 1727.7 cm^{-1}. The last band was already present after deposition but seemed to grow with irradiation. Upon prolonged UV photolysis employing a 280-nm low-pass filter, additional weak bands were observed at 1781 and 1761 cm^{-1}. After annealing the already photolyzed matrix, all these bands diminished or disappeared, and two bands at 1766 and 1759 cm^{-1} with numerous weaker features at 1750.2, 1748.1, 1738.9, 1735.9, and 1719 cm^{-1} appeared. In the experiments with $^{18}O_3$, the principal features shifted to 1742.9, 1715.4, 1708.3, and 1695.8 cm^{-1}, respectively, and when CD_2Br_2 was used as starting material, the bands were shifted to 1746.2, 1719.2, 1696.1, and 1686 cm^{-1}.

Growth Behavior of the Products. A series of photolysis experiments without a filter were performed after several irradiation periods (i) to find primary and secondary products, (ii) to compare reactivity of bromine and chlorine compounds,

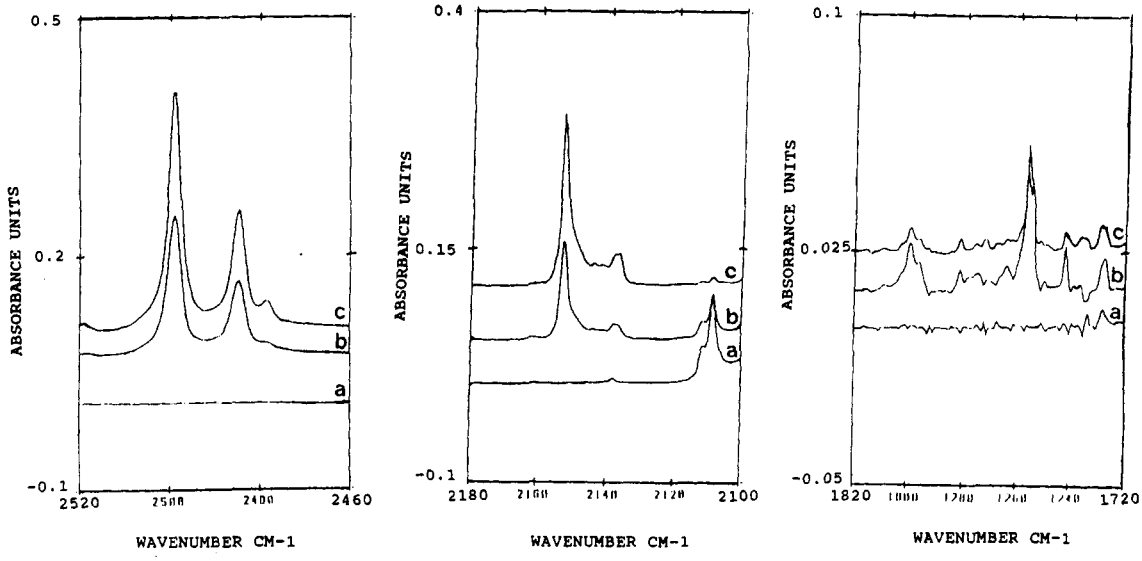

Figure 3. Detailed FTIR spectra of CH_2Br_2 and ^{16}O atom matrix reaction products in the 2520–2460-, 2180–2100-, and 1820–1720-cm^{-1} regions: (a) after deposition of $CH_2Br_2/O_3/Ar$ = 1/2/800 mixture, (b) after irradiation with a medium-pressure mercury lamp filtered at 280 nm for 1 h, and (c) after irradiation as above for 8 h.

TABLE IV: Main Absorptions (cm^{-1}) Formed after Medium-Pressure Mercury Lamp Irradiation of Argon Matrices Containing Natural or Isotopic Ozone and Deuterated Methylene Bromide[a]

$CH_2Br_2 + {}^{16}O_3$	$CH_2Br_2 + {}^{18}O_3$	$CD_2Br_2 + {}^{16}O_3$	assignment
2499.3 (0.25)	2499.1	1794.9	ν(HBr), $(HBr)_2$···CO
2484.8 (0.13)	2485.0	1784.8	
2153.1 (0.16)	2140.3	2154.1	ν(CO), $(HBr)_2$···CO
1799.5 (0.02)	1742.9	1746.2	ν(C=O), HBrCO
1772.8 (0.03)			
1771.4 (0.003)			
1756.3 (0.04)	1715.4	1719.2	ν(C=O), BrH···HBrCO
1754.9 (0.03)			
1742.5 (0.01)	1708.3	1696.1	ν(C=O), H_2CO
1727.7 (0.01)	1695.8	1686.0	ν(C=O), HBr···H_2CO

[a] In parentheses are peak height absorbance values for the $CD_2Br_2 + {}^{16}O_3$ reaction; irradiation time: 4 h.

and (iii) to examine the possibility of an isotopic effect. The photodissociation of ozone depends upon the position and power of the lamp. Hence, the growth of the species was measured relative to the ozone destruction rate. Furthermore, comparison of bromine and chlorine reactivity was made in the same experiment from a 1:1 mixture of CH_2Cl_2 and CH_2Br_2. In the same way, an accurate detection of a possible isotopic effect was performed using a 1:1 mixture of CH_2Cl_2 and CD_2Cl_2.

CH_2Cl_2 + $CH_2Br_2/O_3/Ar$. Figure 4 clearly illustrates that, for the two species, two different groups of bands can be extracted from the spectra. The first one appearing in the carbonyl region showed first an increase and subsequently a decrease in intensity, whereas the second one in the 2000–3000-cm^{-1} region reached a nearly stationary state after the total depletion of ozone with, however, a weak decrease of the 2499- and 2153-cm^{-1} bands and a weak increase for the 2811- and 2157-cm^{-1} absorptions. These two distinct behaviors suggest that the second group of product bands could arise from secondary chemistry initiated by photolysis of carbonyl products. Furthermore, experimental curves show that the concentration versus photolysis time behavior is slightly different for dichloromethane and dibromomethane. The results will be discussed quantitatively later.

CH_2Cl_2 + $CD_2Cl_2/O_3/Ar$. Figure 5 presents the relative intensities of the characteristic product bands at 2811.2, 1751.3 cm^{-1} (parent molecule CH_2Cl_2) and at 2035.4, 1724.4 cm^{-1} (parent molecule CD_2Cl_2) obtained after different irradiation times of a $CH_2Cl_2/CD_2Cl_2/O_3/Ar$ (1/1/2/1000) mixture. If we take account of the fact that the absorption coefficient ratio for H/D stretching mode is about 2 but nearly the same for C=O bands,

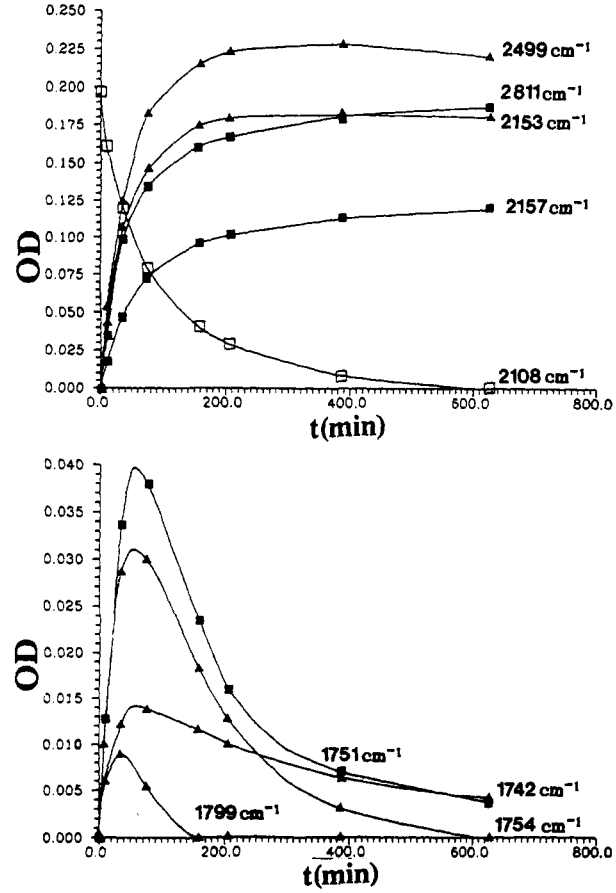

Figure 4. Time evolution of the main products obtained from a mixture of CH_2Cl_2 and CH_2Br_2 with O_3 ($CH_2Cl_2/CH_2Br_2/O_3/Ar$ = 1/1/2/1000) under irradiation with an unfiltered medium-pressure mercury lamp: (■) experimental points relative to CH_2Cl_2 as parent molecule and (▲) experimental points relative to CH_2Br_2 as parent molecule.

the observed results suggest an equal abundance of the carbonyl species and a similar photolysis behavior when both CH_2Cl_2 and CD_2Cl_2 are used as parent molecules.

Reaction with Ground-State Atomic Oxygen. In order to determine whether the different observed reaction products arrived with both ^3P and ^1D atomic oxygen, an experiment was performed where a mixture $CH_2Cl_2/CH_2Br_2/O_3/Ar$ in the ratio 1/1/2/1000 was irradiated for 8 h with light from a Xenon lamp filtered by a 360-nm cut-off filter. Figure 6 compares the spectrum with previous spectra obtained when $CH_2Cl_2 + O_3$ and $CH_2Br_2 + O_3$

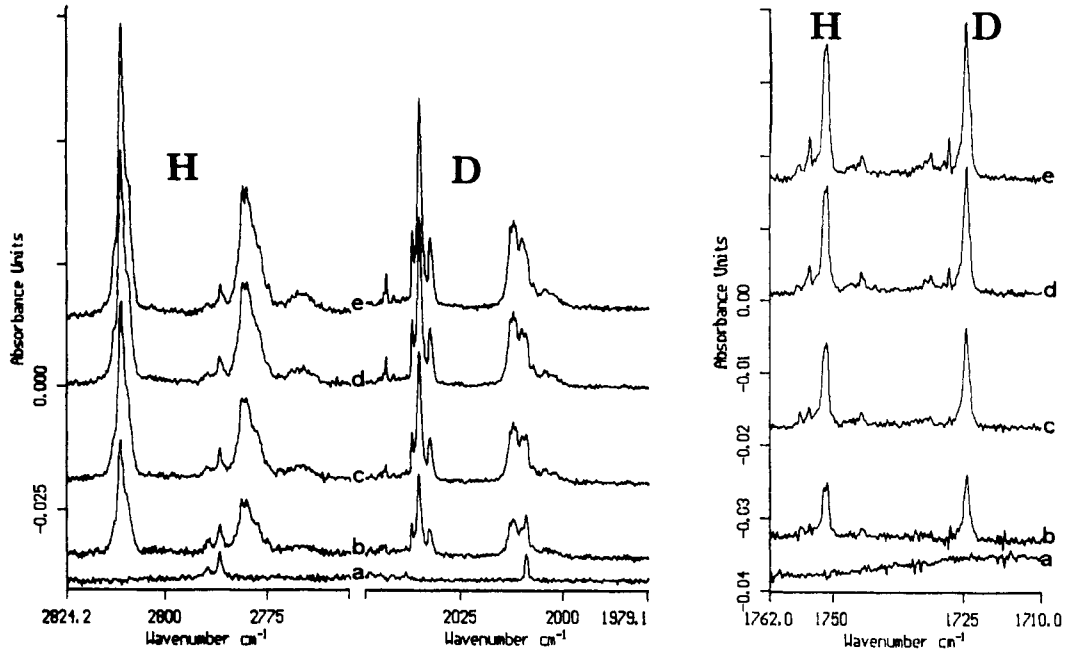

Figure 5. Comparison of the evolution of the products with the time of irradiation (unfiltered medium-pressure mercury lamp) in 2800–1980-cm^{-1} and 1760–1710-cm^{-1} regions after deuteration of the parent molecule: $CH_2Cl_2/CD_2Cl_2 = 1$, CH_2Cl_2, $CD_2Cl_2/O_3/Ar = 1/2/1000$. Irradiation times: (a) 0, (b) 1 h, (c) 2 h, (d) 3 h, 40 min, (e) 5 h. According to the parent molecules, products are labeled either H or D.

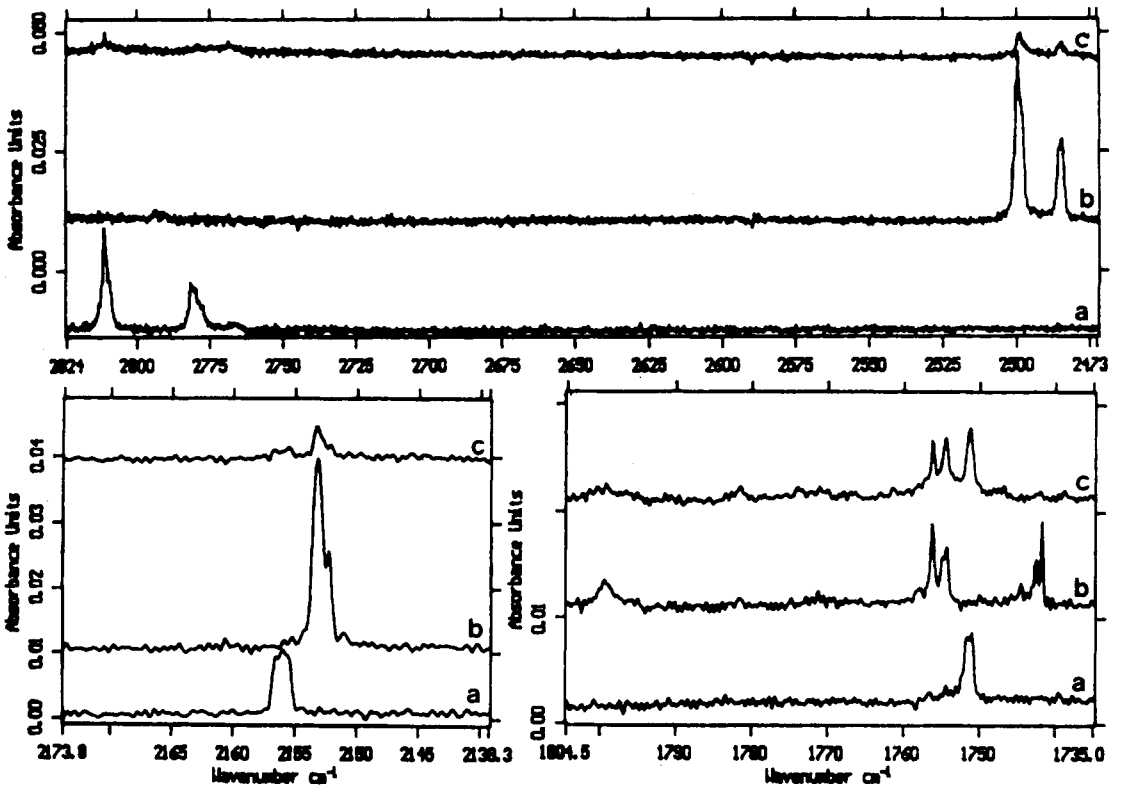

Figure 6. Comparison of the spectra in the key regions after irradiation of: (a) $CH_2Cl_2/O_3/Ar$ (1/1/1000) mixture with medium-pressure mercury lamp without filter, (b) $CH_2Br_2/O_3/Ar$ (1/1/1000) mixture with medium-pressure mercury lamp without filter, (c) $CH_2Cl_2/CH_2Br_2/O_3/Ar$ (0.5/0.5/1/1000) mixture with Xenon lamp and cut-off filter WG 360. Irradiation times: (a) 40 min, (b) 10 min, (c) 7 h, 30 min. All spectra are recorded at 11 K.

matrix mixtures were photolyzed with the full light of the medium-pressure mercury lamp. Two observations deserve attention: (i) in the carbonyl region the band at 1742 cm^{-1} was not observed and (ii) in the 2800–2150-cm^{-1} region bands previously reported appeared as traces.

Oxygen Matrix. In an attempt to gain information on the reaction intermediates, an experiment on the photolysis of CH_2Cl_2 in a solid O_2 matrix, which is a strongly oxidizing environment, was carried out with the full light of the mercury lamp (CH_2Cl_2/O_2 1/1000). As mentioned in the Experimental Section, irradiation of solid O_2 below 280 nm produces ozone and $O(^3P)$ with subsequent secondary photolysis of ozone. Although the product yield was considerably lower than that in the previous experiments, similar product absorptions (compared to argon matrix experiments) appeared in the three key regions after photolysis. They were respectively observed at 2804.6, 2771.3; at 2159.6; and at 1754.4, 1753.0, 1749.5 cm^{-1}. The triplet in the carbonyl region was sensitive to temperature increase but with a trend different from that observed in the argon matrix: the lower component grew with the temperature whereas the higher component disappeared. In addition, new bands not seen in argon were observed at 1724.4, 1391.3, and 1100.0 cm^{-1}.

Discussion

Vibrational Spectra of Parent Molecules. The bands observed for the parent halides are in agreement with values from the vapor-phase[9,10] and matrix isolation studies.[12,14,15] Some of the observed bands showed isotopic splitting due to the natural abundance of chlorine and bromine isotopes ($^{35}Cl^{35}Cl \approx 57\%$, $^{35}Cl^{37}Cl \approx 37\%$, $^{37}Cl^{37}Cl \approx 6\%$, $^{79}Br^{79}Br \approx 26\%$, $^{81}Br^{81}Br \approx 24\%$, and $^{79}Br^{81}Br \approx 50\%$). This have previously been described for the ν_3 and ν_9 bands.[9,11,12] For comparison, we have included the calculated isotopic shifts in Tables I and II (see later). Due to the isotopic mixing, the ν_5 mode (A_2, IR inactive) is also observed in the spectra. In a recent report of the IRMI spectrum of CH_2Cl_2,[13] the ν_2 mode was assigned to a band at 1455 cm^{-1} while the 1428-cm^{-1} band was ascribed to the overtone, $2\nu_3$. Because of the better resolution in our experiments, we observed an isotopic splitting of the 1450-cm^{-1} band (1453.5, 1451.5, and 1448.7 cm^{-1}) while the 1428.4-cm^{-1} band shows no such splitting. We therefore assign the latter band to the ν_2 mode (CH_2 scissoring), for which the normal coordinate calculations show no isotopic splitting. The bands around 1450 cm^{-1} are instead ascribed to a combination of the two CCl stretching modes, $\nu_3 + \nu_9$ (B_2). This interpretation is also in agreement with the thorough vapor-phase study by Duncan *et al.*[9]

The analogous combination band in CH_2Br_2 is observed at 1226 cm^{-1}, also in good agreement with the literature, where this is reported as the strongest combination band.[10]

The vibrational wavenumbers for methylene chloride as well as the isotopic shifts and a general harmonic force field have been presented by Duncan *et al.*[19] In order to calculate the vibrational fundamentals and isotopic shifts in methylene bromide, we adopted the electron diffraction structure[20] and scaled the methylene chloride force field by the inverse square of the distances for the stretching constants and the stretch–stretch interactions and by the inverse distances for the bending constants and the stretch–bend interactions.

Identification of Compounds Formed by UV Photolysis. Identification and vibrational assignments of the two product sets recognized from their growth behavior (Figure 4) will be considered separately. The first one was characterized by very weak, photosensitive bands in the carbonyl region, whereas the second one appeared in the 2800–2000-cm^{-1} region as stronger absorptions.

Carbonyl Products. After photolysis of the CH_2Cl_2/O_3 mixture, a triplet band was observed at 1751, 1753, and 1756 cm^{-1} with a 42-cm^{-1} ^{18}O shift and a 27-cm^{-1} deuterium shift. This group of bands has been interpreted as due to the C=O stretching vibration in formyl chloride complexed by HCl. This agrees with previous identification of the complex in solid nitrogen by Nelander.[21] The multiplicity of the C=O band also observed in nitrogen suggests a possible different relative orientation of the complex forming molecules. The increase in intensity of the bands with the temperature is surprising. It is perhaps an indication of recombination in the matrix cage of photolytic fragments not identified.

Photolysis of the CH_2Br_2/O_3 matrix gave three new bands in the carbonyl stretching region at 1799, 1756–1754, and 1742 cm^{-1}. As can be seen in Figure 4, their different growth behavior indicates that they belong to three distinct species. The band at 1742 cm^{-1} shifts to 1696 cm^{-1} upon deuteration and is due to $\nu_{C=O}$ of free formaldehyde.[22] The position of the doublet at 1756–1754 cm^{-1} and its isotopic shift upon deuteration (1719 cm^{-1}) resemble the situation in the CHOCl···HCl complex and have tentatively been assigned to the CHOBr···HBr complex. The identification of the 1799-cm^{-1} band is less straightforward. However, the apparent isotopic shifts observed with $^{18}O_3$ and under deuteration indicate the presence of one hydrogen atom and one oxygen atom, and the absorption is therefore tentatively ascribed to free HCOBr. Formyl bromide has not been matrix isolated previously, but the IR spectrum of it in the vapor phase was recently obtained by Niki.[23] The carbonyl vibration of formyl bromide was observed at 1799.5 cm^{-1} in Fermi resonance with $2\nu_6$ at 1774.2 cm^{-1}. It shifts to 1746.2 cm^{-1} in the DCOBr species. The product yield in our experiments is probably too small for an accurate observation of the $2\nu_6$ band, although a narrow feature at 1771.3 cm^{-1} which grows in concert with the 1799-cm^{-1} band could be due to this overtone. Furthermore, the shift observed for isotopic substitution with $^{18}O_3$ is larger than the one observed for the HCOBr···HBr complex, but it is of the same order of magnitude if it is calculated from the 1789-cm^{-1} position, the position for the fundamental carbonyl band vibration in the vapor phase.

Second Set of Products. With dichloromethane as the parent molecule, new bands appeared at 2811 and 2781 cm^{-1}. Upon deuteration, these band shifted to 2035 and 2012 cm^{-1} and can unambiguously be assigned to the HCl stretching vibration of the $(HCl)_2$···CO aggregate.[24,25] The corresponding CO absorption was observed at 2156.6 and 2155.6 cm^{-1} for the parent and deuterated molecules, respectively.

The results for dibromomethane have been interpreted in the same fashion. The new bands at 2499, 2485 (shoulder at 2479 cm^{-1}), and 2153–2152 cm^{-1} for the parent molecule, shifting to 1795, 1785, and 2154 cm^{-1} with the deuterated bromide and to 2499, 2485, and 2140 cm^{-1} with $^{18}O_3$ precursor, have been assigned to the $(HBr)_2$···CO complex. Perchard *et al.*[24] observed the same bands in a study of various HBr/CO complexes, but their interpretation was somewhat different. In experiments with CD_2Br_2/O_3, the DBr stretching modes of the $(DBr)_2$···CO complex fall in the carbonyl region (1795 and 1785 cm^{-1}). Growth curves show them as final products, however, and they are therefore easily distinguished from the carbonyl intermediates.

Kinetic Studies. In order to obtain quantitatively significant results for the abundance of the different products as a function of the time and to determine accurately primary and secondary species, kinetic studies were performed using the experimental curves of Figure 4 within the framework used in our previous studies.[7] Reactions are considered as first-order processes and can be schematically represented by

$$O_3 \xrightarrow{k_0} O_2 + O$$

$$(CH_2X_2, O_3) \xrightarrow{k_1} P \xrightarrow{k_2} S$$

where (CH_2X_2, O_3) refers to the fraction N^0 of CH_2X_2 and O_3 in neighboring "reactive sites", P to primary products, and S to secondary products.

The rate constant k_0 of ozone depletion can be easily calculated from $(O_3)^t = (O_3)^0 \exp(-k_0 t)$. The abundances of P and S are respectively given by

$$N_p = \frac{N^0 k_1}{k_1 - k_2}[\exp(-k_2 t) - \exp(-k_1 t)] = \alpha[\exp(-k_2 t) - \exp(-k_1 t)] \quad (1)$$

$$N_s = N^0\left[1 + \frac{k_2 \exp(-k_1 t) - k_1 \exp(-k_2 t)}{k_1 - k_2}\right] \quad (2)$$

Numerical values of α, k_1, and k_2 for carbonyl products were obtained by a least-squares fit of experimental curves using the Microsoft Excel program. Values were adjusted in order to minimize the residual sum of squares between the calculated N_p and observed N_p values. Results are summarized in Table V and compared to the average dissociation rate constant k_0 of ozone. k_1 values are of the same order of magnitude for the formation of all carbonyl compounds, suggesting that the reaction is principally governed by ozone photodissociation. Secondary photolysis of COHCl···HCl appears slightly more rapid than that

TABLE V: Comparison between Kinetic Rate Constants (in min^{-1}) at 10 K for Formation (k_1) and Dissociation (k_2) of the Primary Products Obtained from Photolysis of a CH_2Cl_2/CH_2Br_2/O_3/Ar (1/1/2/1000) Mixture by Medium-Pressure Mercury Lamp[a]

parent molecule	products	k_1	k_2	k_1/k_Q
CH_2Cl_2	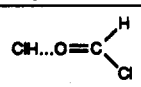	2.9×10^{-2}	7×10^{-3}	1.2
	$CO\cdots(HCl)_2$	2.5×10^{-2}		1
CH_2Br_2	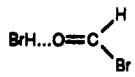	3.0×10^{-2}	7.5×10^{-3}	1.2
		3.3×10^{-2}	3.0×10^{-2}	1.3
		3.0×10^{-2}	2.0×10^{-3}	1.2
	$CO\cdots(HBr)_2$	2.5×10^{-2}		1

[a] In this experiment, the average depletion rate constant of ozone, k_0, was found equal to 2.5×10^{-2} min^{-1}.

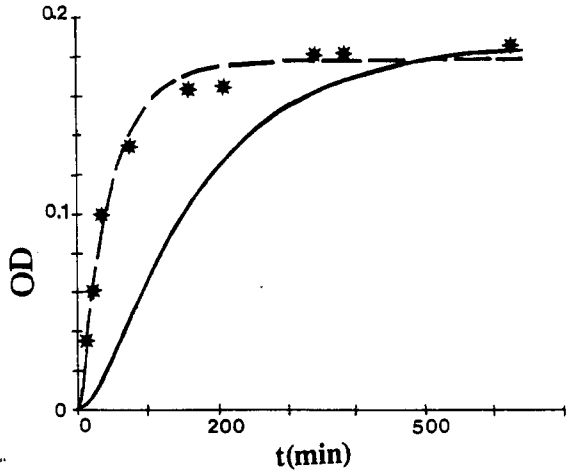

Figure 7. Comparison between calculated curves from different equations for the time evolution of of the $CO\cdots(HCl)_2$ product: (—) calculated curve using eq 2 with $k_1 = 2.9 \times 10^{-2}$ min^{-1} and $k_2 = 7.0 \times 10^{-3}$ min^{-1}, (- - -) calculated curve using eq 3, and (★) experimental points.

of COHBr···HBr, whereas the dissociation of free COHBr appears nearly as fast as its formation.

Photolysis of these carbonyl compounds is assumed to produce secondary products. In particular, COHX···HX can lead to $CO\cdots(HX)_2$ as final products and experimental growth curves of these species are expected to be fitted by eq 2 using the previously calculated k_1 and k_2 values for each parent molecule. As illustrated in Figure 7, the experimental growth curve for $CO\cdots(HCl)_2$ complex formation does not comply with that for CHOCl···HCl formation ($k_1 = 2.9 \times 10^{-2}$ min^{-1} and $k_2 = 7.0 \times 10^{-3}$ min^{-1}). In fact, the experimental curve can be approximated by a single-exponential curve of the form $N_s = N^0(1 - \exp(-k_1 t))$.

TABLE VI: Predicted $\Delta H°$ for $CH_2X_2 + O$ Reactions (X = Cl, Br) in kJ/mol

reaction	X = Cl STO-3G	X = Cl 3-21G	X = Cl 3-21G*	X = Br STO-3G
$CH_2X_2 + O(^1D) = CH_2O + X_2$	−247	−280	−278	−320
$CH_2X_2 + O(^1D) = CHOX + HX$	−358	−420	−430	−403
$CH_2X_2 + O(^1D) = COX_2 + H_2$	−330	−300	−333	−347
$CH_2X_2 + O(^3P) = CH_2O + X_2$	127	51	53	54
$CH_2X_2 + O(^3P) = CHOX + HX$	16	−89	−99	−29
$CH_2X_2 + O(^3P) = COX_2 + H_2$	44	32	−2	27

The same applies to the $CO\cdots(HBr)_2$ growth curve, with a similar rate constant of ca. 2.5×10^{-2} min^{-1} ($k_1/k_0 = 1$). This suggests that $CO\cdots(HX)_2$ complexes are formed both as primary and secondary products of the $CH_2X_2 + O_3$ reaction.

Photolytic Process. *Reaction Pathways.* From kinetic studies, the observed product distribution points to two pathways for the initial step of the $CH_2Cl_2 + O_3$ reaction and three channels for that of the $CH_2Br_2 + O_3$ reaction (Chart I).

In the matrix cage, the HX molecule appears complexed either by the formyl-halogenated or CO species, although in the case of the CH_2Br_2 parent molecule free formyl bromide also seems to be present. Upon further photolysis, HXCO···HX complexes decompose to $(HX)_2\cdots CO$ species whereas H_2CO dissociates to CO and H_2, as expected.[20] Only the first pathway leading to XHCO molecules is observed with atomic oxygen both in the excited and ground state. Ground-state atomic oxygen is not reactive enough to produce H_2CO or $CO\cdots(HX)_2$. Table VI summarizes *ab initio* calculated $\Delta H°$ values for different possible routes.[26] Although there is some dispersion among the results obtained with the different basis sets, it is clear that CHOX, COX_2, CO, and CH_2O all would result from the reactions with $O(^1D)$ and also that CHOX formation should be a possible product from a reaction with $O(^3P)$. COX_2 is not observed in our experiments, and CH_2O is only observed with CH_2Br_2 as the parent molecule, this last observation being the most striking result in comparing the CH_2Cl_2/O_3 and the CH_2Br_2/O_3 reactions. Before excluding this reaction path for the methylene chloride reaction, the possibility that $H_2CO\cdots HCl$ is formed and then rapidly destroyed needs to be examined. According to Nelander,[23] when nitrogen matrices containing formaldehyde and chlorine were photolyzed through a $NiSO_4$ solution, the formaldehyde complex decreased rapidly in intensity, and formation of HClCO was observed. Although this possibility cannot entirely be ruled out in our experiments, it seems unlikely for two reasons: (i) no traces of $O{=}CH_2$ or $O{=}CH_2\cdots HCl$ species were observed in our spectra and (ii) the growth curve of HClCO:HCl has an exponential behavior without a sigmoidal contour at short times, suggesting that it cannot also be a secondary species produced by photodissociation of a $H_2CO\cdots Cl_2$ complex.

Mechanism. The primary step of the formyl halide formation might be one of the three following possibilities: (i) insertion of an oxygen atom into the C–H bond, (ii) abstraction followed by bond cleavage leading to the product, and (iii) addition to a carbon atom giving a five-centered excited intermediate.

The insertion of an oxygen atom in an excited state into the C–H bond has already been observed; in particular, by photolyzing

CHART I

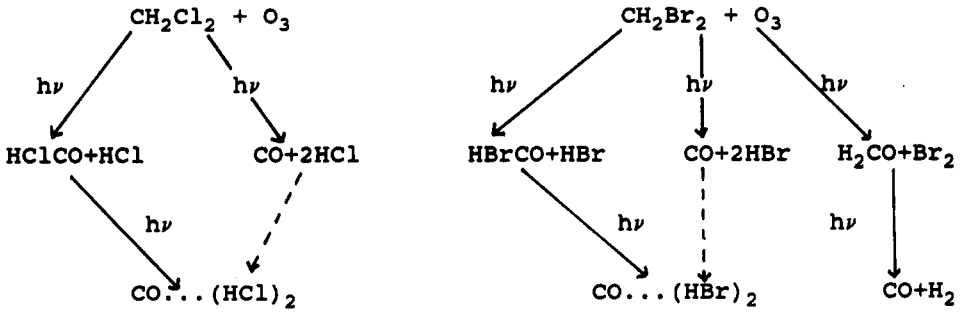

TABLE VII: Comparison of Reaction Products for Reactions between Various Halomethanes and Either O(¹D) or O(³P) Oxygen Atoms

system	primary products	
	O(¹D)	O(³P)
$CBrCl_3 + O$		
$CFCl_3 + O$		–
$CCl_4 + O$		*a*
$CBr_4 + O$		*a*
$CHCl_3 + O$	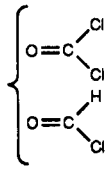	
$CH_2Cl_2 + O$		
$CHBr_3 + O$	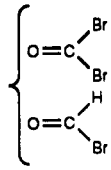	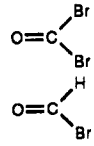
$CH_2Br_2 + O$	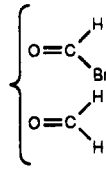	
$CH_3Br + O$		

[a] Experiment not performed.

an O_3–CH_4 mixture in liquid argon the excited CH_3OH intermediate was evident.[27] However, this insertion is unlikely when atomic oxygen is in its ground state.[28] In our experiments, both O(³P) and O(¹D) react in the same way, and insertion into the CH bond seems to be ruled out. The absence of any isolated intermediate makes it difficult to determine which of the two other pathways is the major one, although the two bands observed in the oxygen matrix (1391.3 and 1100.0 cm^{-1}) assigned to the O_2H species[29] could be an indication of H abstraction followed by bond cleavage leading to the product.

Formation of CH_2O observed only in the reaction between CH_2Br_2 and O(¹D) probably arises from a different mechanism. In this case, insertion of O(¹D) into a C–Br or a C–H bond to form a vibrationally excited intermediate which undergoes two rearrangements before its fast dissociation is a possibility.

Table VII shows a summary of the different products found in our laboratories for the reaction between halocarbons and O(³P) and O(¹D). In all cases, carbonyl compounds are the main primary products. In the absence of a hydrogen atom in the parent molecule, two halogen atoms are abstracted. As expected, the C–Br (ca. 210 kJ/mol) bond is more easily broken than the C–Cl bond (ca. 370 kJ/mol) while the C–F bond (ca. 530 kJ/mol) is not broken at all. Irradiation of a $CCl_4/O_3/Ar$ or $CBr_4/O_3/Ar$ mixture leads to the expected product COX_2. For the halogenated hydrogen species, the major route observed for the reaction with both O(³P) and O(¹D) is the abstraction of HX species. This abstraction leads to O=CHX from CH_2X_2 and to O=CX_2 from CHX_3. Thus, the great affinity between the H and X atoms favors this abstraction of HX occurring also with O(³P).

Acknowledgment. Our sincere thanks to Dr. A. J. Barnes for reading and improving the manuscript. One of us (L.S.M.) thanks the NAVF (Norway) for an invitation to the Department of Chemistry of Oslo University (Professor P. Klaboe). In Paris, our sincere thanks to Dr. R. Levant for helping in the calculations performed with the Microsoft Excel program.

References and Notes

(1) The Airborne Antarctic Ozone Experiment. *J. Geophys. Res.* **1989**, *94*, (D9, 30 August; D14, 30 November).
(2) The first Airborne Arctic Stratospheric Exedition (AASE-I). *Geophys. Res. Lett.* **1990**, *17* (Number 4, March).
(3) WMO, Global ozone research and monitoring project. *Report. no. 25*, 1991.
(4) Lasson, E.; Klaboe, P.; Nielsen, C. J. *Air Pollution Res. Rep.* **1991**, *42*, 79.
(5) Wayne, R. P. *Chemistry of the Atmospheres*, 2nd ed.; Oxford Scientific Publications, 1991.
(6) Abdelaoui, O.; Schriver, L.; Schriver, A. *J. Mol. Struct.* **1992**, *268*, 335.
(7) Schriver, L.; Gauthier-Roy, B.; Carrère, D.; Schriver, A.; Abouaf-Marguin, L. *Chem. Phys.* **1992**, *163*, 357.
(8) Schriver, L.; Abdelaoui, O.; Schriver, A. *J. Phys. Chem.* **1992**, *96*, 8069.
(9) Duncan, J. L.; Nivellini, G. D.; Tullini, F. *J. Mol. Spectrosc.* **1986**, *118*, 145.
(10) Dennen, R. S.; Piotrowski, E. A.; Cleveland, F. F. *J. Chem. Phys.* **1968**, *49*, 4385.
(11) King, S. T. *J. Chem. Phys.* **1968**, *49*, 1321.
(12) Kelsall, B. J.; Andrews, L. *J. Mol. Spectrosc.* **1983**, *97*, 362.
(13) Mikulec, J.; Cerny, C. *Spectrochim. Acta* **1987**, *43A*, 849.
(14) Andrews, L.; Prochaska, F. T.; Ault, B. S. *J. Am. Chem. Soc.* **1979**, *101*, 9.
(15) Young, N. A.; Speicer, M. D. *J. Mol. Struct.* **1990**, *222*, 77.
(16) Spoliti, M.; Nunziante-Cesaro, S.; Mariti, B. *J. Chem. Phys.* **1973**, *59*, 985.
(17) Andrews, L.; Spiker, R. C., Jr. *J. Phys. Chem.* **1972**, *76*, 3208.
(18) Green, D. W.; Erwin, K. M. *J. Mol. Spectrosc.* **1981**, *88*, 51.
(19) Duncan, J. L.; Lawie, D. A.; Nivellini, G. D.; Tullini, F.; Fergusson, A. M.; Harper, J.; Tonge, K. H. *J. Mol. Spectrosc.* **1987**, *121*, 294.
(20) Beagley, B.; Brown, D. P.; Freeman, J. M. *J. Mol. Struct.* **1974**, *20*, 315.
(21) Strandman-Long, L.; Nelander, B.; Nord, L. *J. Mol. Struct.* **1984**, *117*, 217.
(22) Diem, M.; Lee, E. K. C. *J. Phys. Chem.* **1982**, *86*, 4507.
(23) Yarwood, G.; Niki, H.; Maker, P. D. *J. Phys. Chem.* **1991**, *95*, 4773.
(24) Perchard, J. P.; Cipriani, J.; Silvi, B.; Maillard, D. *J. Mol. Struct.* **1983**, *100*, 317.
(25) Andrews, L.; Arlinghaus, R. T.; Johnson, G. L. *J. Chem. Phys.* **1983**, *78*, 6348.
(26) Trucks, G. W.; Foresman, J. B.; Schlegel, H. B.; Raghavachari, K.; Robb, M.; Binckley, J. S.; Gonzalez, C.; Defrees, D. J.; Fox, D. J.; Whiteside, R. A.; Seeger, R.; Melius, C. F.; Baker, J.; Martin, R. L.; Kahn, L. R.; Stewart, J. J. P.; Topiol, S.; Pople, J. A. *Gaussian 90*, Revision I; Gaussian Inc.: Pittsburgh PA, 1990.
(27) Demore, W. B.; Raper, O. F. *J. Chem. Phys.* **1967**, *46*, 2500.
(28) Luntz, A. C. *J. Chem. Phys.* **1980**, *73*, 1143.
(29) Milligan, D. E.; Jacox, M. E. *J. Chem. Phys.* **1963**, *38*, 2627.
(30) Escribano, R.; Orza, J. M.; Montero, S.; Domingo, C. *Mol. Phys.* **1979**, *37*, 361.